Complex Frequency Propagation along Transmission Lines

Ignacio Ponce, *IEEE Member*, and Federico Milano, *IEEE Fellow*

School of Electrical and Electronic Engineering
University College Dublin, Ireland

***Abstract*—The paper proposes a Complex Frequency Continuum Model (CFCM) to represent the propagation of voltage dynamics along transmission lines. The proposed CFCM is based on the concept of Complex Frequency (CF), recently proposed by the second author. This model removes the assumption of small voltage magnitude an phase angles in the transmission system, which are the basis for a Linear Continuum Model (LCM) also recently proposed by the second author. The paper identifies two major differences between the CFCM and the LCM. On the one hand, the former captures the nonlinearity of the spatial rate of change of the CF. On the other hand, it recognizes the cross-dependence between the real and imaginary parts of the CF along a line. Time-domain simulations are carried out in a case study whose transmission system operates highly loaded, and the performance of the CFCM and the LCM are compared to a PLL-based estimation of the CF at different points of a line. Simulation results verify the accuracy of the proposed approach, and show the errors introduced by the LCM in estimating the CF at an intermediate point of a line.**

I. Introduction

The increase of penetration of converter-interfaced devices is changing how power systems are modeled, studied, controlled, and operated [1]–[3]. A critical aspect of this transition is the need for an appropiate definition, modelling and analysis of local frequency dynamics [4]–[6]. A pioneer work in this field is the Frequency Divider Formula [7], which provides a way to estimate the frequency at every bus of the grid.

It is also relevant to investigate how voltage and frequency dynamics propagate across the transmission system [8], [9]. A well-known model that represents the grid as a distributed continuum proposed in the seminal work [10]. Therein, the electromechanical wave theory was used to represent frequency variations as travelling waves. However, this model requires strong approximations such as linearizing the system, lossless lines, and a ficticious distribution of the parameters of the generators throughout the network. Further research have ellaborated in partially removing the assumptions of [10], investigated its properties and exploited its potential in protection and control applications [11]–[15].

A recent work has provided an alternative continuum-based approach based on the Frequency Divider Formula [16]. The key difference with respect to [10] is that the model proposed in [16] does not require to distribute the synchronous machines since it works directly in the original system. Consequently, the inconsistent fast dynamics or modes that appear with the electromechanical wave approach are removed. However, the model in [16] still requires neglecting voltage magnitude variations and assuming slight phase differences between consecutive buses. Under these circumstances, the authors show that the frequency distributes linearly throughout the transmission system. Nevertheless, the simplifications on which it is based are questionable under high-loading conditions, or following faults critical to voltage or rotor angle stability.

The frequency dynamics propagation is one side of the problem. The complete voltage dynamics involve also the rate of change of its magnitude. In this vein, the novel concept of the complex frequency (CF) have been defined recently in [17], allowing to conveniently represent the interactions between complex power injections and voltage dynamics in magnitude and phase. Recent works have shown the importance of this term for the correct interpretation and analysis of the frequency variations, as well as promising applications in power system modelling, control and state estimation [18]–[21]. In this work, we describe how the CF propagates along transmission lines, thus providing a more complete and general approach than those published so far.

The primary contribution of the paper is to provide a systematic approach to describe the voltage dynamics propagation along transmission lines, namely, in magnitude and frequency, through a general and compact formulation.

The remainder of the document is organized as follows. Section II presents the Linear Continuum Model (LCM), which is an extended version of the model in [16] including a analogue equation for estimating the real part of the CF. Section III presents the proposed Complex Frequency Continuum Model (CFCM), and shows that it is a generalization of the FD-based model. Section IV presents a comparison of the performance of the LCM and the CFCM in a benchmark system using time-domain simulations. Finally, conclusions and future work are outlined in Section V.

II. Linear Continuum Model

As mentioned in the introduction, previous works have found that under negligible voltage magnitude variations and minor phase differences between two consecutive buses the frequency distributes linearly throughout a line [16]:

$$\omega(x) = \frac{x\omega_0 + (1-x)\omega_l}{l}\,, \tag{1}$$

where $x \in \mathbb{R} \mid x \in [0, l]$ is the position of a point in a line of length l, ω_0 and ω_l are the (known) frequencies at

the endpoints of the line. The spatial rate of change of the frequency is constant and equal to:

$$\frac{\partial \omega(x)}{\partial x} = \frac{\omega_0 - \omega_l}{l}\,. \tag{2}$$

The underlying assumption that leads to the expressions above is that voltage magnitude variations are negligible ($v_0 \approx v_l \approx$ const). However, since we are interested in assessing the spatial continuity of the CF, i.e., $\overline{\eta} = \rho + j\omega$, rather than neglecting it, we assume an analogue linear expression for ρ to complete the LCM. Thus:

$$\rho(x) = \frac{x\rho_0 + (1-x)\rho_l}{l}\,, \tag{3}$$

$$\frac{\partial \rho(x)}{\partial x} = \frac{\rho_0 - \rho_l}{l}\,, \tag{4}$$

or, equivalently:

$$\boxed{\overline{\eta}(x) = \frac{x\overline{\eta}_0 + (1-x)\overline{\eta}_l}{l}} \tag{5}$$

Equation (5) provides a linear estimation of the CF of the voltage at any intermediate point of the line x only in terms of the CF at both ends (boundary conditions) and l. This model is compared with the Complex Frequency Continuum Model that is described in the following section and that removes the abovementioned assumptions.

III. Proposed Complex Frequency Continuum Model

A. Derivation

Consider a transmission line of length l (km) which connects bus 0 and bus l. The voltage at both ends is known and denoted $\overline{v}_0$ and $\overline{v}_l$. Similarly, their CF is also considered known thus acting as a boundary condition. They are denoted as $\overline{\eta}_0$ and $\overline{\eta}_l$. Let $x \in \mathbb{R} \mid x \in [0, l]$ be the position of a point in the line (km) measured from bus 0 to bus l. The line is represented through the well-known PI model of lumped parameters with series impedance $\overline{Z}$ and shunt susceptance $B/2$ at both ends. Finally, we assume that at any intermediate point of the line, the model is split into two smaller PI blocks, where the parameters are divided proportionally to x. Figure 1 illustrates the model described above. In the figure, the following notation is used:

$$\overline{z} = \frac{\overline{Z}}{l}\,, \qquad b = \frac{B}{l}\,. \tag{6}$$

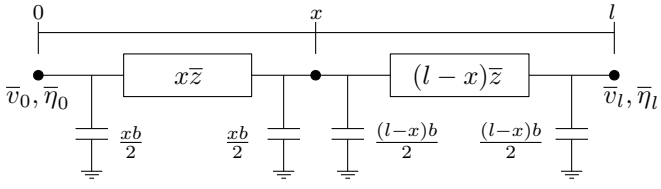

Fig. 1: Model of the line.

The model above allows us to define a function for the voltage of the line $\overline{v}(x):\ \mathbb{R} \to \mathbb{C}$ with boundary conditions at both ends of the line: $\overline{v}(0) = \overline{v}_0$, $\overline{v}(l) = \overline{v}_l$. The function $\overline{v}(x)$ is found starting from the KCL at x:

$$0 = \frac{\overline{v}(x) - \overline{v}_0}{x\overline{z}} + \frac{\overline{v}(x) - \overline{v}_l}{(l-x)\overline{z}} + \overline{v}(x) j\frac{B}{2}\,, \tag{7}$$

from where $\overline{v}(x)$ is obtained:

$$\overline{v}(x) = \frac{(l-x)\overline{v}_0 + x\overline{v}_l}{1 - j\frac{B}{2}\overline{z}(l-x)x}\,. \tag{8}$$

Similarly, we define the function of the complex frequency of the line $\overline{\eta}(x):\ \mathbb{R} \to \mathbb{C}$ as:

$$\overline{\eta}(x) = \frac{\dot{\overline{v}}(x)}{\overline{v}(x)}\,, \tag{9}$$

where $\dot{\overline{v}}(x)$ represents the time derivative of the voltage of the line. At both ends of the line: $\overline{\eta}(0) = \overline{\eta}_0$, $\overline{\eta}(l) = \overline{\eta}_l$.

Replacing (8) into (9):

$$\overline{\eta}(x) = \left(\frac{(l-x)\overline{v}_0\overline{\eta}_0 + x\overline{v}_l\overline{\eta}_l}{1 - j\frac{B}{2}\overline{z}(l-x)x}\right)\left(\frac{1 - j\frac{B}{2}\overline{z}(l-x)x}{(l-x)\overline{v}_0 + x\overline{v}_l}\right)$$

$$\Rightarrow \boxed{\overline{\eta}(x) = \frac{(l-x)\overline{v}_0\overline{\eta}_0 + x\overline{v}_l\overline{\eta}_l}{(l-x)\overline{v}_0 + x\overline{v}_l}} \tag{10}$$

Equation (10) defines the CF of the voltage at any intermediate point of the line x only in terms of the voltages and CF at both ends (boundary conditions) and l.

Next, we study the partial derivative $\frac{\partial \overline{\eta}(x)}{\partial x}$, which carries the information of how the CF of the voltage continuously varies throughout the transmission system. The calculation begins as follows:

$$\begin{aligned}\frac{\partial \overline{\eta}(x)}{\partial x} = &\frac{(\overline{v}_l\overline{\eta}_l - \overline{v}_0\overline{\eta}_0)((l-x)\overline{v}_0 + x\overline{v}_l)}{((l-x)\overline{v}_0 + x\overline{v}_l)^2} \\ &- \frac{(\overline{v}_l - \overline{v}_0)((l-x)\overline{v}_0\overline{\eta}_0 + x\overline{v}_l\overline{\eta}_l)}{((l-x)\overline{v}_0 + x\overline{v}_l)^2}\,.\end{aligned} \tag{11}$$

Simplifying the expression given by (11) leads to:

$$\frac{\partial \overline{\eta}(x)}{\partial x} = (\overline{\eta}_l - \overline{\eta}_0)\frac{\overline{v}_l\overline{v}_0 l}{((l-x)\overline{v}_0 + x\overline{v}_l)^2}\,, \tag{12}$$

or, equivalently:

$$\frac{\partial \overline{\eta}(x)}{\partial x} = \frac{(\overline{\eta}_l - \overline{\eta}_0)l}{\left(\frac{\overline{v}_0}{\overline{v}_l} + \frac{\overline{v}_l}{\overline{v}_0} - 2\right)x^2 + 2l\left(1 - \frac{\overline{v}_0}{\overline{v}_l}\right)x + l^2\frac{\overline{v}_0}{\overline{v}_l}}\,. \tag{13}$$

At both ends, the expression yields:

$$\frac{\partial \overline{\eta}(x)}{\partial x}_{|x=0} = \frac{(\overline{\eta}_l - \overline{\eta}_0)}{l}\left(\frac{\overline{v}_l}{\overline{v}_0}\right) \tag{14}$$

$$\frac{\partial \overline{\eta}(x)}{\partial x}_{|x=l} = \frac{(\overline{\eta}_l - \overline{\eta}_0)}{l}\left(\frac{\overline{v}_0}{\overline{v}_l}\right)\,. \tag{15}$$

If we denote the complex nonlinear part of (13) as $\overline{h}(x)$:

$$\overline{h}(x) = \frac{l}{\left(\frac{\overline{v}_0}{\overline{v}_l} + \frac{\overline{v}_l}{\overline{v}_0} - 2\right)x^2 + 2l\left(1 - \frac{\overline{v}_0}{\overline{v}_l}\right)x + l^2\frac{\overline{v}_0}{\overline{v}_l}} \tag{16}$$

Then:

$$\frac{\partial \overline{\eta}(x)}{\partial x} = (\overline{\eta}_l - \overline{\eta}_0)\overline{h}(x)\,. \tag{17}$$

Finally, splitting the real and imaginary parts of (17) we obtain the spatial rate of change of ρ and ω:

$$\frac{\partial \rho(x)}{\partial x} = (\rho_l - \rho_0)\Re\{\overline{h}(x)\} - (\omega_l - \omega_0)\Im\{\overline{h}(x)\}\,, \quad (18)$$

$$\frac{\partial \omega(x)}{\partial x} = (\omega_l - \omega_0)\Re\{\overline{h}(x)\} + (\rho_l - \rho_0)\Im\{\overline{h}(x)\}\,. \quad (19)$$

Equations (18) and (19) show two substantial differences with the linear continuum model:

1) **The complex frequency does not vary linearly throughout the line**. This is a consequence of the fact that $\frac{\partial \rho(x)}{\partial x}$ and $\frac{\partial \omega(x)}{\partial x}$ depend on the position x along the line.
2) **There is a cross dependence between $\boldsymbol{\rho}$ and $\boldsymbol{\omega}$**. This is a consequence of the fact that $\overline{h}(x)$ is complex. Thus, $\omega(x)$ is not only a function of ω_0 and ω_l, but also ρ_0 and ρ_l.

B. Simplifications

We examine how the complex nonlinear term $\overline{h}(x)$ simplifies considering commonly made assumptions that usually hold in normal operating conditions. These are (i) the voltage magnitude at both ends of the line is approximately the same, i.e., $v_0 \approx v_l = v$; and (ii) the angle difference is slight enough to approximate the trigonometric functions as follows: $\sin(\theta_0 - \theta_l) \approx (\theta_0 - \theta_l)$, and $\cos(\theta_0 - \theta_l) \approx 1$. Under these assumptions, the coefficient accompanying x^2 in (16) vanishes:

$$\left(\frac{\overline{v}_0}{\overline{v}_l} - \frac{\overline{v}_l}{\overline{v}_0} - 2\right) \approx \cos(\theta_0 - \theta_l) + \cos(\theta_l - \theta_0) - 2 + ... \\ ... + j\sin(\theta_0 - \theta_l) + j\sin(\theta_0 - \theta_l)\,, \quad (20)$$

$$\left(\frac{\overline{v}_0}{\overline{v}_l} - \frac{\overline{v}_l}{\overline{v}_0} - 2\right) \approx 2\cos(\theta_0 - \theta_l) - 2 = 0\,. \quad (21)$$

Thus:

$$\overline{h}(x) \approx \frac{l}{2l\left(1 - \frac{\overline{v}_0}{\overline{v}_l}\right)x + l^2\frac{\overline{v}_0}{\overline{v}_l}}\,. \quad (22)$$

Again, adopting the assumptions above simplifies to:

$$\overline{h}(x) \approx \frac{1}{l + j(\theta_0 - \theta_l)(2x - l)}\,. \quad (23)$$

Note that $(\theta_0 - \theta_l)(2x - l) \ll l$ for $x \in [0, l]$, therefore:

$$\overline{h}(x) \approx \frac{1}{l}\,. \quad (24)$$

Finally,

$$\frac{\partial \rho(x)}{\partial x} \approx \frac{\rho_l - \rho_0}{l}\,, \quad (25)$$

$$\frac{\partial \omega(x)}{\partial x} \approx \frac{\omega_l - \omega_0}{l}\,, \quad (26)$$

which are consistent with the linear continuum model described in Section II. Therefore, the CFCM is a generalization of the LCM. In conclusion, the higher the magnitude and angle differences between voltages at both ends of a line, the higher the error between the simplified and the proposed continuum models. Cases of particular interest in this work are long transmission lines or high-loading operating conditions.

IV. Case study

The Kundur's two-area benchmark system is used to implement and compare the LCM and the proposed CFCM [22]. Figure 2 shows a single-line diagram of the system including the values of some relevant variables of the operating point studied. We are particularly interested in the line connecting buses 7 and 9, which links the two areas of the system, each of them composed of two synchronous generators.

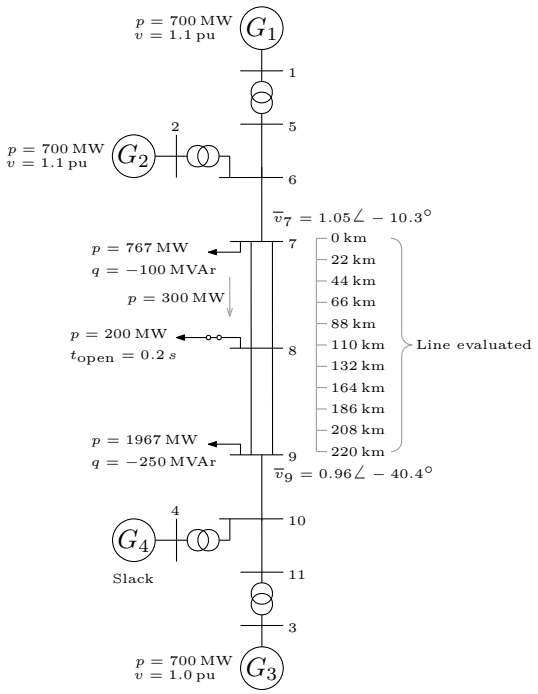

Fig. 2: Single line diagram of Kundur's two-area system [22].

A time domain simulation is performed given the initial conditions shown in Fig. 2. The load connected at bus 8 is suddenly disconnected at $t = 0.2$ s. The frequency deviation from the COI ($\Delta\omega$) and the rate of change of the voltage magnitude (ρ) are evaluated at different points of the line (steps of 10% of the total length). We compare a PLL measurement at that point[1], an estimation through the LCM (equation (5)) and the calculation given by the proposed CFCM (equation (10)). The results for ω and ρ at the 30%, 50% and 70% of the line are shown in Figs. 3 to 8. While the CFCM matches the direct PLL measurement at every location, the LCM performs with a noticeable error. This is due to the operating point being such that there is a non-negligible voltage difference between the two endpoints of the line, both in magnitude and phase. The higher this difference, the higher the error introduced with the LCM.

Finally, we calculate the Root Mean Squared Error (RMSE) between both models and the PLL measurement at the points of the line evaluated. This is done considering the first four

[1]Note that even though PLLs are commonly used to estimate the time derivative of the angle, i.e., $\dot{\theta} = \omega$, an analogue architecture can also be used to calculate the time derivative of any other algebraic variable. In this case, it is used to get the time derivative of the voltage's magnitude, and thus ρ.

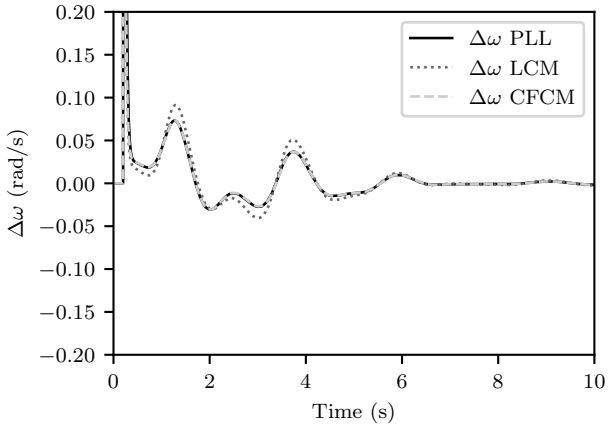

Fig. 3: Frequency deviation at 30% of the line: PLL, LCM and CFCM.

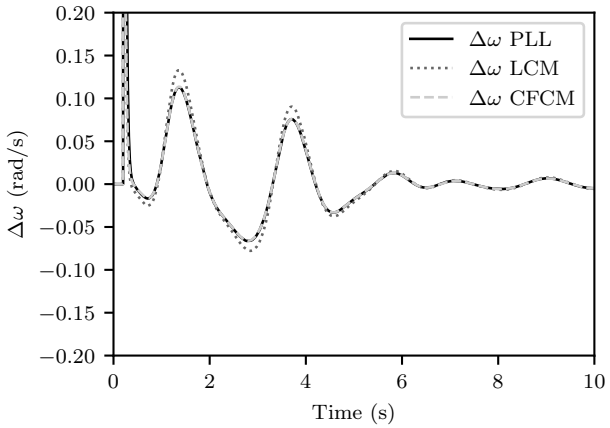

Fig. 4: Frequency deviation at 50% of the line: PLL, LCM and CFCM.

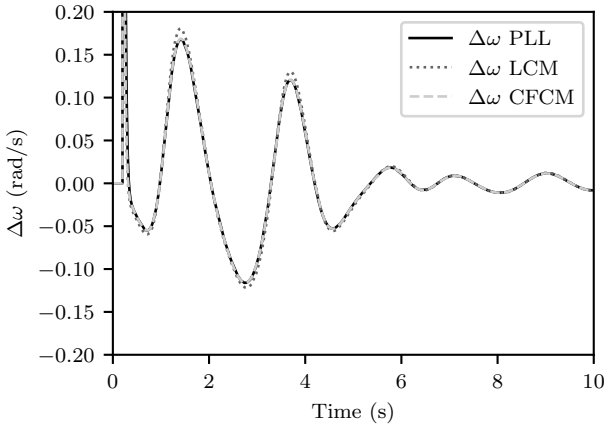

Fig. 5: Frequency deviation at 70% of the line: PLL, LCM and CFCM.

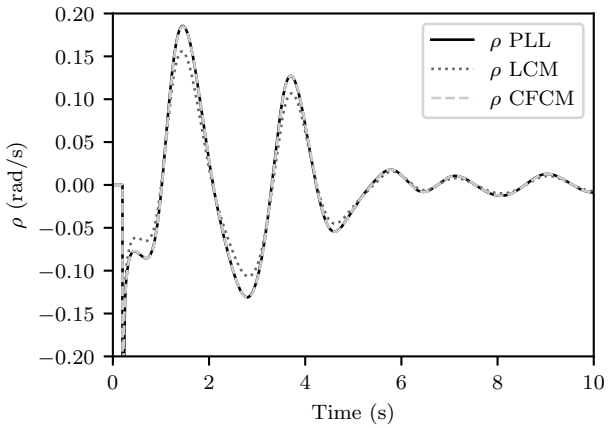

Fig. 6: Rocov deviation at 30% of the line: PLL, LCM and CFCM.

seconds after the event. The results for ω and ρ are shown in Figs. 9 and 10, respectively. As expected, the CFCM's error is nearly null. In contrast, the LCM's error is noticeable and, interestingly, more prominent for ρ than ω. The error curve has a quadratic shape, with the maximum error at an intermediate point, not necessarily right in the middle of the line.

V. Conclusion

The paper proposes a continuum model based on the concept of complex frequency, namely CFCM, which describes the propagation of voltage dynamics through transmission lines, both in magnitude and angle. The proposed CFCM captures the nonlinearity of the spatial rate of change of the CF along a line and recognizes the cross dependence between ρ and ω. The paper also shows that the CFCM is a generalization of the LCM since the former simplifies to the latter under proper approximations. The case study shows that, under high-loading operating conditions, the CF along the line estimated through the CFCM matches a PLL-based estimation. On the other hand, the LCM shows a significant error, higher for ρ than for ω. The shape of the error resemble a quadratic behavior, and the maximum occurs at an intermediate point around the middle of the line. Future work will elaborate on the consequences of considering each model and its possible applications.

Acknowledgments

This work is supported by the Sustainable Energy Authority of Ireland (SEAI) by funding I. Ponce and F. Milano under project FRESLIPS, Grant No. RDD/00681.

References

[1] N. Hatziargyriou *et al.*, "Definition and classification of power system stability – revisited & extended," *IEEE Transactions on Power Systems*, vol. 36, no. 4, pp. 3271–3281, 2021.

[2] F. Milano, F. Dörfler, G. Hug, D. J. Hill, and G. Verbič, "Foundations and challenges of low-inertia systems (invited paper)," in *Power Systems Computation Conference (PSCC)*, pp. 1–25, 2018.

[3] M. N. H. Shazon, Nahid-Al-Masood, and A. Jawad, "Frequency control challenges and potential countermeasures in future low-inertia power systems: A review," *Energy Reports*, vol. 8, pp. 6191–6219, 2022.

[4] H. Kirkham, W. Dickerson, and A. Phadke, "Defining power system frequency," in *IEEE PES General Meeting (PESGM)*, pp. 1–5, 2018.

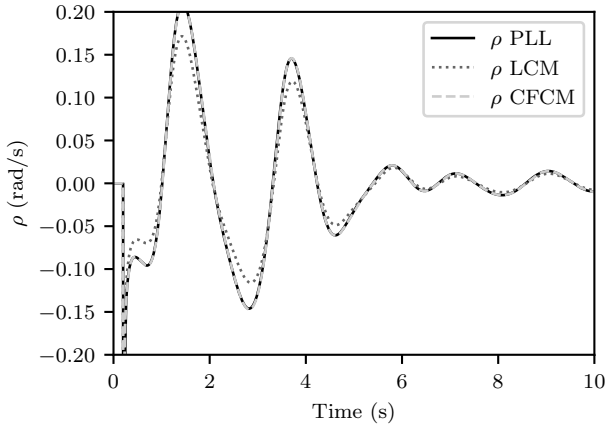

Fig. 7: Rocov deviation at 50% of the line: PLL, LCM and CFCM.

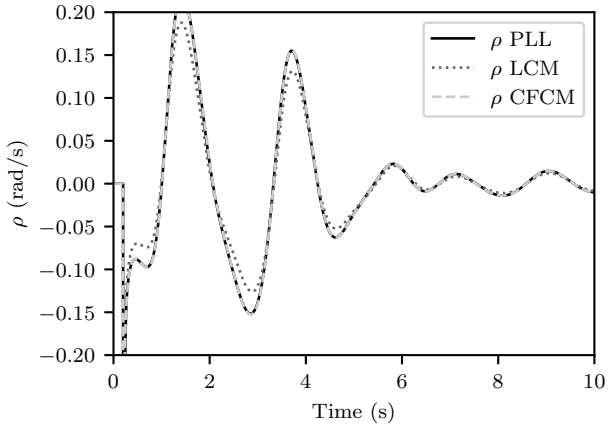

Fig. 8: Rocov deviation at 70% of the line: PLL, LCM and CFCM.

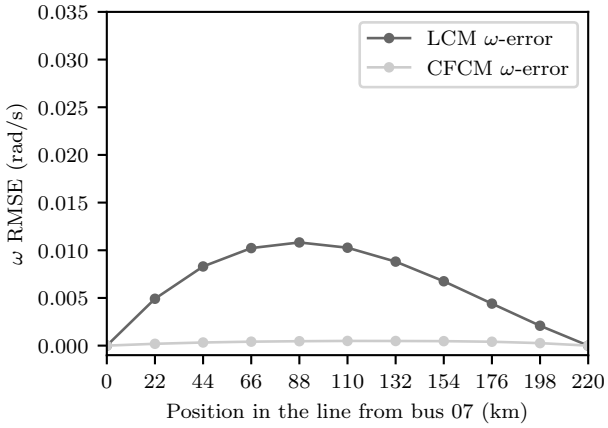

Fig. 9: Root mean squared error for the frequency: LCM and CFCM.

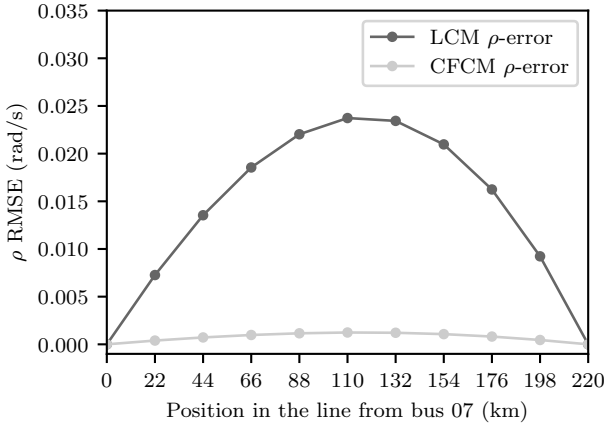

Fig. 10: Root mean squared error for the Rocov: LCM and CFCM.

[5] G. Frigo, A. Derviškadić, and M. Paolone, "Impact of fundamental frequency definition in ipdft-based pmu estimates in fault conditions," in *IEEE 10th International Workshop on Applied Measurements for Power Systems (AMPS)*, pp. 1–6, 2019.

[6] F. Milano and Á. Ortega, *Frequency Variations in Power Systems: Modeling, State Estimation, and Control*. IEEE Press, Wiley, 2020.

[7] F. Milano and Á. Ortega, "Frequency divider," *IEEE Transactions on Power Systems*, vol. 32, no. 2, pp. 1493–1501, 2017.

[8] T. Li, G. Ledwich, Y. Mishra, J. H. Chow, and A. Vahidnia, "Wave aspect of power system transient stability—part i: Finite approximation," *IEEE Transactions on Power Systems*, vol. 32, no. 4, pp. 2493–2500, 2017.

[9] T. Li, G. Ledwich, Y. Mishra, J. H. Chow, and A. Vahidnia, "Wave aspect of power system transient stability—part ii: Control implications," *IEEE Transactions on Power Systems*, vol. 32, no. 4, pp. 2501–2508, 2017.

[10] A. Semlyen, "Analysis of disturbance propagation in power systems based on a homogeneoue dynamic model," *IEEE Transactions on Power Apparatus and Systems*, vol. PAS-93, no. 2, pp. 676–684, 1974.

[11] J. Thorp, C. Seyler, and A. Phadke, "Electromechanical wave propagation in large electric power systems," *IEEE Transactions on Circuits and Systems I: Fundamental Theory and Applications*, vol. 45, no. 6, pp. 614–622, 1998.

[12] M. Parashar, J. Thorp, and C. Seyler, "Continuum modeling of electromechanical dynamics in large-scale power systems," *IEEE Transactions on Circuits and Systems I: Regular Papers*, vol. 51, no. 9, pp. 1848–1858, 2004.

[13] H. Zhang, F. Shi, Y. Liu, and V. Terzija, "Adaptive online disturbance location considering anisotropy of frequency propagation speeds," *IEEE Transactions on Power Systems*, vol. 31, no. 2, pp. 931–941, 2016.

[14] T. Bi, J. Qin, Y. Yan, H. Liu, and K. E. Martin, "An approach for estimating disturbance arrival time based on structural frame model," *IEEE Transactions on Power Systems*, vol. 32, no. 3, pp. 1741–1750, 2017.

[15] D. Huang, J. Qin, H. Liu, J. H. Chow, J. Zhao, T. Bi, L. Mili, and Q. Yang, "An analytical method for disturbance propagation investigation based on the electromechanical wave approach," *IEEE Transactions on Power Systems*, vol. 36, no. 2, pp. 991–1001, 2021.

[16] G. Tzounas, I. Dassios, and F. Milano, "Frequency divider as a continuum," *IEEE Transactions on Power Systems*, vol. 37, no. 6, pp. 4970–4973, 2022.

[17] F. Milano, "Complex frequency," *IEEE Transactions on Power Systems*, vol. 37, no. 2, pp. 1230–1240, 2022.

[18] D. Moutevelis, J. Roldan-Perez, M. Prodanovic, and F. Milano, "Taxonomy of power converter control schemes based on the complex frequency concept," *arXiv preprint arXiv:2209.11107*, 2022.

[19] F. Milano, B. Alhanjari, and G. Tzounas, "Enhancing frequency control through rate of change of voltage feedback," *IEEE Transactions on Power Systems*, pp. 1–4, 2023.

[20] X. He, V. Häberle, and F. Dörfler, "Complex-frequency synchronization of converter-based power systems," 2022.

[21] D. Moutevelis, J. Roldán-Pérez, M. Prodanovic, and F. Milano, "Design of virtual impedance control loop using the complex frequency approach," in *2023 IEEE Belgrade PowerTech*, pp. 1–6, 2023.

[22] P. Kundur, N. Balu, and M. Lauby, *Power System Stability and Control*. EPRI power system engineering series, McGraw-Hill Education, 1994.